

# Hot Ductility Study of HAYNES® 282® Superalloy

Joel Andersson<sup>1,2</sup>, Göran Sjöberg<sup>1,2</sup> and Mahesh Chaturvedi<sup>3</sup>

<sup>1</sup>Volvo Aero Corporation

Materials Technology Department, Trollhättan, 461 81, Sweden

<sup>2</sup>Chalmers University of Technology, Department of Materials and Manufacturing Technology, Göteborg, 412 96, Sweden

<sup>3</sup>University of Manitoba, Department of Mechanical and Manufacturing Engineering, Winnipeg, R3T 5V6, Canada

Keywords: Haynes 282, hot ductility

## Abstract

The hot ductility of the newly developed Haynes 282 alloys has been investigated in different solution heat treatments conditions using the Gleeble weld thermal simulation method. The ultimate purpose of this study is to assess the feasibility of using this new alloy for the large aircraft engine structures. The strengthening response on cooling down from the solution heat treatment at different temperatures between 1121 and 1135°C with cooling rates of ~0.3°C/s was considerable (~100 HV increase compared with the as-received condition of HV215) and which may jeopardize weldability, not unexpectedly, in  $\gamma'$  hardening alloys. Initial hardness had no or minor influence on hot ductility. Still, the coarse grains achieved by a solution heat treatment heating at 1135°C-2hrs, ASTM 1 compared to initial ASTM 5 did lower the hot ductility.

## Introduction

A new wrought Gamma-prime strengthened Ni – based superalloy, Haynes 282, is intended for high temperature structural applications [1]. It also has potential as a filler material for weld repair of more potent  $\gamma'$  strengthened superalloys (i.e. Alloy 939, Rene-41 and Waspaloy) in hot structural applications [2]. A challenge in the development of superalloy for structural applications to be used in the temperature range of 800 – 900°C is to produce an alloy capable of good creep strength and good thermal stability and with resistance to strain age cracking during post weld heat treatment as well as resistance to hot cracking during the welding operation. Generally, increasing the amounts of the  $\gamma'$  hardening elements (Al, Ti and Ta) potentially raise the risk for strain age cracking (SAC) whereas some specific trace elements and eutectic formers (B, P, S, Zr, C and Nb) severely induce hot cracks [3, 4, 5, 6].

A similar alloy, Waspaloy, commonly used in aerospace applications has marginal creep strength and thermal stability above 800°C and SAC susceptibility is high. Rene-41, another,  $\gamma'$  strengthened alloy even more related to Haynes 282 than Waspaloy, possesses excellent creep strength but poor thermal stability and low resistance to SAC [1]. A comparison in chemical composition between these three alloys is shown in table 1.

Table 1. Nominal Composition of Several Wrought Gamma - Prime Alloys (wt. %)

Alloy	Ni	Cr	Co	Mo	Ti	Al	Fe	Mn	Si	C	B	Other
282	BAL	20	10	8.5	2.1	1.5	1.5*	0.3*	0.15*	0.06	0.005	-
Waspaloy	BAL	19	13.5	4.3	3	1.5	2*	0.1*	0.15*	0.08	0.006	Zr-0.05
Rene-41	BAL	19	11	10	3.1	1.5	5*	0.1*	0.5*	0.09	0.006	-

\*Maximum

The most significant differences in chemical composition are the Ti and Mo contents where the decreased amount of Ti lowers the amount of  $\gamma'$  whereas an increased amount of Mo increases the solid solution hardening – creep properties at high temperatures.

The heat treatment of Haynes 282 alloy is carried out in three steps - first a high temperature solution treatment at 1121-1149°C for 30min to 2hrs followed by rapid cooling or water quenched. This is a solution heat treatment where carbides may also dissolve which depends on the choice of temperature and time. The solution heat treatment is followed by a two step aging treatment; 1010°C-2hrs air cooled (AC) and 788°C-8hrs AC both with the purpose of for carbide precipitation and  $\gamma'$  (790°C-8hrs) precipitation.

It is recommended that the solution heat treatment (1121-1149°C for 30min-2hrs) also is performed prior to welding followed by as rapid cooling as possible to minimize precipitation. A post weld solution heat treatment is also necessary for restoring properties in complex weldments [7].

From SAC point of view the Haynes 282 alloy is believed to be less susceptible compared with Waspaloy and Rene-41 (due to the lower content of Ti). This is reflected in the well-known Prager-Shira WRC (welding research council) diagram which states that the Al+Ti content should be kept below 6 atomic % to avoid problems with SAC [3].

The susceptibility to hot cracking, on the other hand, also depends on the alloying elements but in a more complex way during the actual solidification through the influence on the primary and secondary phases involved. The way these phases behave in terms of liquation and solidification during the weld thermal cycle is crucial for the hot cracking tendency. The primary  $\gamma$  and the  $\gamma'$  as well as the secondary phases  $M_{23}C_6$  and  $M_6C$  are all face centered cubic (FCC) in Haynes 282 and do not develop any significant lattice strain during the weld thermal cycle (<2.5%) which is beneficial from welding point of view [8].

A method to investigate the susceptibility for hot cracking in the heat affected zone (HAZ) by liquation cracks is to quantify the elevated temperature ductility measured as the reduction of area by simulating the weld thermal cycle through rapidly heating and cooling of a small sample. This can be done by Gleeble testing which uses resistance heating and by water cooling.

During heating materials usually experience a sharp drop in ductility which is an indication of liquation and finally the ductility drops to zero at the nil ductility temperature (NDT). As the temperature is increased the nil strength temperature (NST) is reached where the material does not possess any strength. When the on-cooling ductility is to be determined the sample is first heated to the NST temperature minus 30 °C before the cooling of the samples to the desired testing temperature. The ductility will recover at low enough temperature, the ductility recovery

temperature (DRT), indicating that the liquid generated at the high temperature has solidified and the material now will be able to resist stresses and strains with a measurable amount of ductility. It goes without saying that the larger the interval between the highest temperature, NST, and the DRT the larger is the risk of hot cracking during welding due to the developing stresses associated with thermal constrain during the cooling down. This interval, i.e. brittle temperature range ( $BTR = NST - DRT$ ), provides a useful tool in ranking different alloys in terms of the susceptibility for hot cracking during welding. It also brings understanding into more basic questions of material research and development [9, 10].

### Experimental

A computer controlled Gleeble 1500-D machine, Figure 1, was used to examine the hot ductility to better understand the welding limits of Haynes 282.

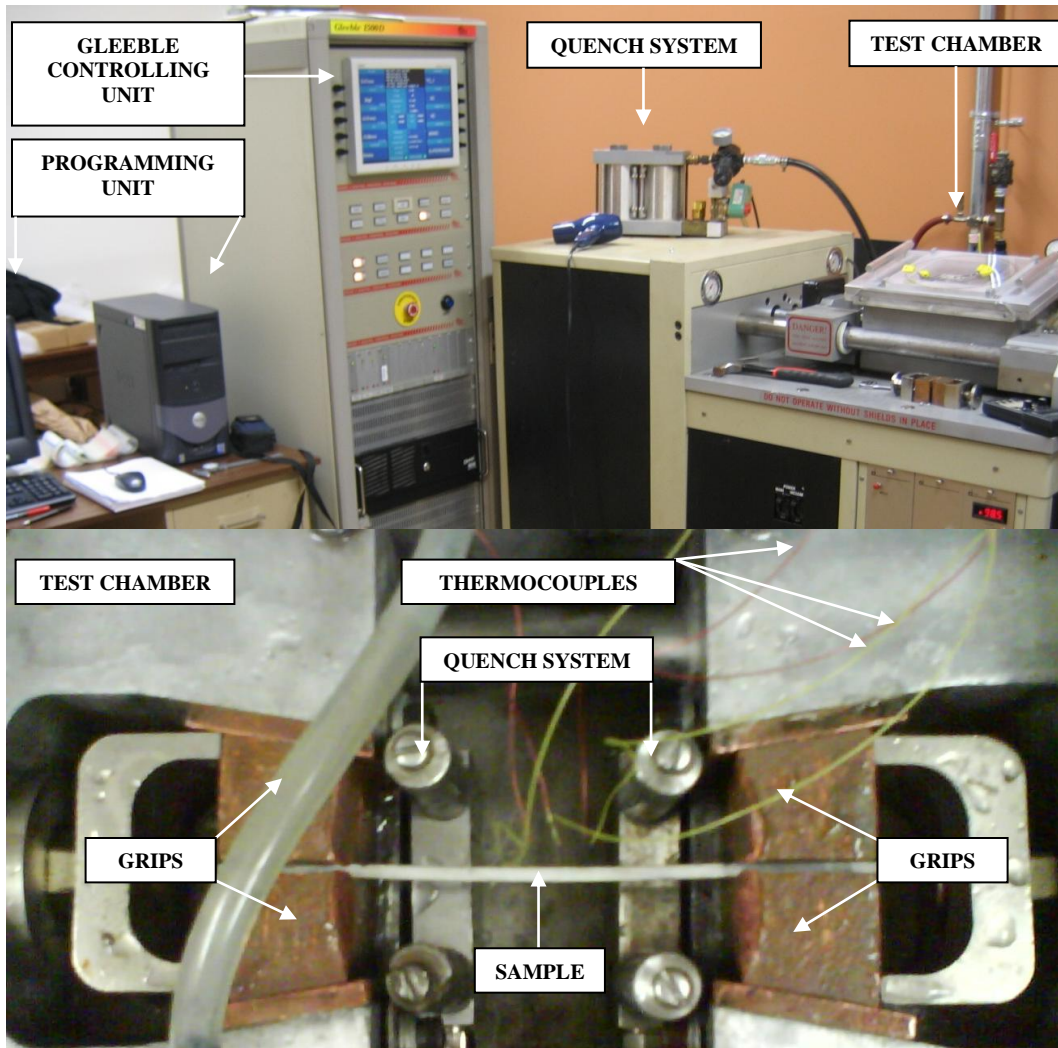


Figure 1. Overview of the Gleeble test setup.

A 3.2mm thick sheet with the chemical composition shown in table 2 was water-jet machined to produce the test specimen geometry in Figure 2. Thermocouples of Pt-type were percussion welded to the central part of the specimens for temperature control.

Table 2. Chemical composition of Haynes® 282® test material (wt. %)

Heat Number	Alloy	Ni	Cr	Co	Mo	Ti	Al	Fe	Mn	C	B	P	S
20825-8354	282	BAL	19.63	10.35	8.56	2.21	1.41	0.35	0.08	0.068	0.004	0.002	0.002

The sheet was delivered in bright annealed condition carried out in a continuous heat treating furnace at 1121-1150°C for about 30min and then quenched to room temperature to minimize precipitation.

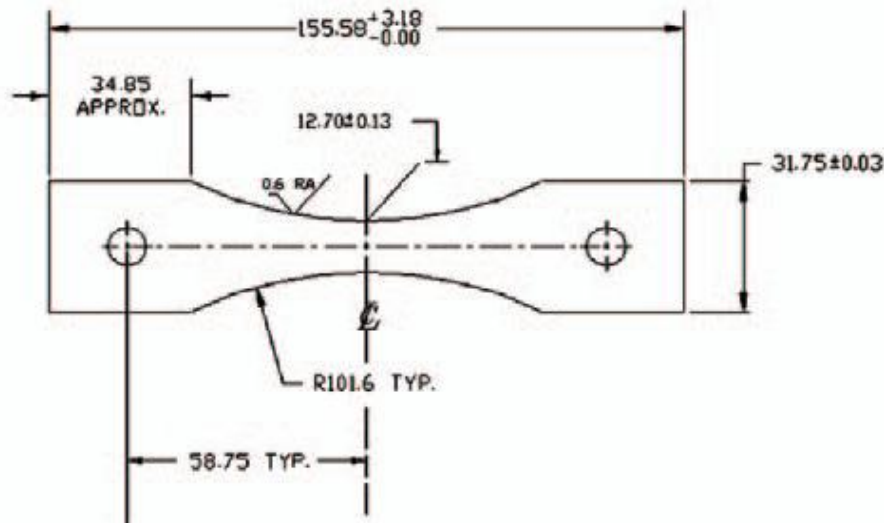


Figure 2. Geometry of Gleeble the test specimens.

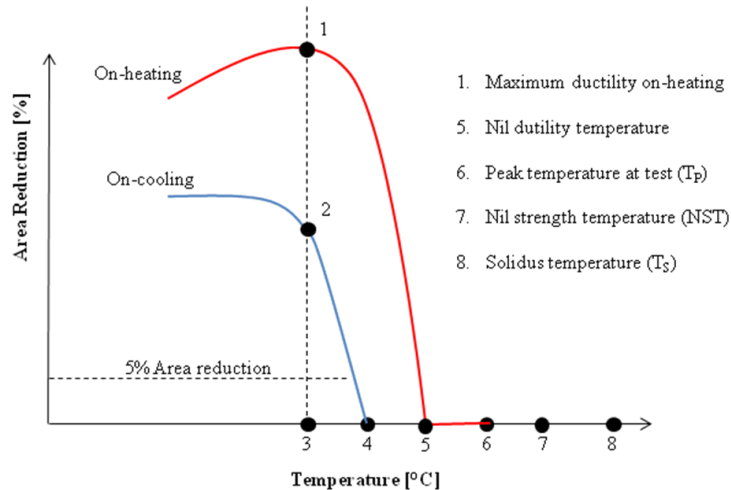
The material was tested in the three following conditions:

1. 1121 to 1149°C-30min quenched to room temperature (as –received).
2. As-received + 1121°C-30min fan argon cooling at >20°C/min to 500°C.
3. As-received + 1135°C-2hrs (to produce coarse grains), fan argon cooling at >20°C/min to 500°C.

The purpose was to see what influence a second solution heat treatment would have on the hot ductility compared with the as-received condition. Of special interest in welding is the affect of coarse grain sizes on hot ductility.

As is schematically shown in Figure 3 [10] the hot ductility characteristics were determined in terms of the Nil Ductility Temperature (NDT), the Ductility Recovery Temperature (DRT) and the Nil Strength Temperature (NST) and as already mentioned in the introductory part of this paper. First, the NST was determined, by using a constant load (100N), to find at what temperature the material cannot sustain any load. This temperature minus 30°C was then taken as the peak heating temperature to be used in the temperature test program for determining the on-cooling ductility. From these measurements the brittle temperature range (BTR), ratio of ductility recovery (RDR), and ductility recover rate (DRR) were determined. This approach to evaluating the susceptibility to hot cracking is a generally accepted procedure [10].

The BTR, the difference between peak temperature (NST-30°C) used for the thermal cycle minus the DRT, is the temperature range wherein the material is sensitive to cracking and possess zero ductility. DRR is the difference between the maximum on-heating ductility and on-cooling ductility whereas RDR is the ratio between the area of the on-heating and on-cooling curves as schematically shown in Figure 3.



DRT: The temperature where 5% area reduction on-cooling is measured.

BTR:  $T_p - DRT$

DRR:  $(2-3)/(1-3) \times 100$

RDR:  $\text{area}(2-3-4)/\text{area}(1-3-5) \times 100$

Figure 3. Schematic representation of Gleeble measurements from the Swedish standard institute [10].

The parameters used for Gleeble testing is shown in table 3.

Table 3. Gleeble parameters used for testing.

Heating rate	111°C/s
Cooling rate	50°C/s
Stroke rate	55mm/s
Holding time at peak temperature	0.03s
Holding time at test temperature	0.03s

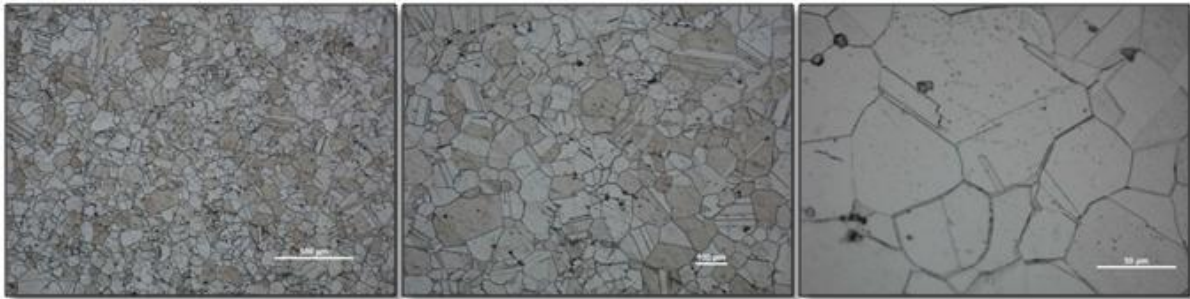
Optical microscopy and Vickers hardness testing (1kg load) were carried out on selected specimens. Grain size was measured according to ASTM E 112. Metallographic preparations were to standard procedures with electrolytic etching in oxalic acid for 3-6s at 4-6V.

## Results

The microstructure, hardness and grain size of the three different conditions are shown in Figure 4. The low hardness shown in the as-received material in comparison the significantly higher hardness (~100HV for 1121°C-30min) indicates that a substantial amount of precipitation has taken place in the subsequent heat treatment. The difference in hardness for the two latter conditions (1121°C-30min and 1135°C-2hrs) is probably due to the difference in grain size (the

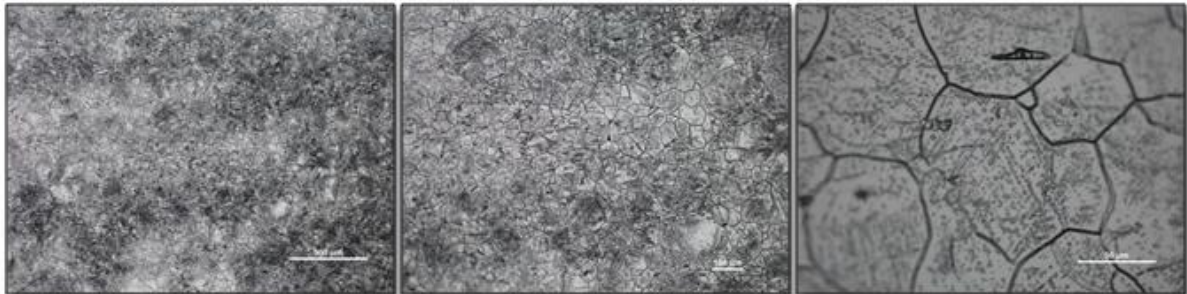
Petch-Hall relation) since the grain size increased significantly, from ASTM 5 to ASTM 1, during the 2 hrs dwell time at 1135°C.

**As-received (1121-1149°C-30 min)**



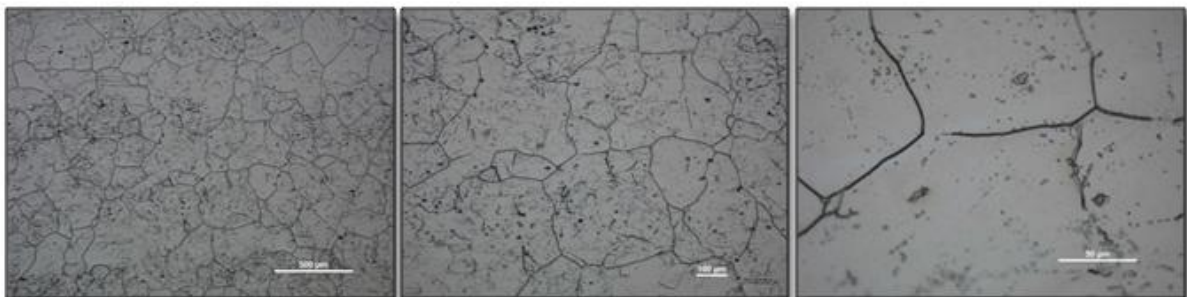
x50    x100    x500  
 Grain size ASTM 5, Average HV 215 (out of 10 indents)

**1121°C-30min**



x50    x100    x500  
 Grain size ASTM 5, Average HV 317 (out of 10 indents)

**1135°C-2hrs**



x50    x100    x500  
 Grain size ASTM 1, Average HV 283 (out of 10 indents)

Figure 4. Microstructure, grain size) and hardness Vickers (HV1) of the as received , 1121°C-30min and 1135°C-2hrs, respectively.

The on-heating and on-cooling hot ductility for each condition is shown in Figure 5-7. A comparison of the hot ductility is shown in Figure 8.

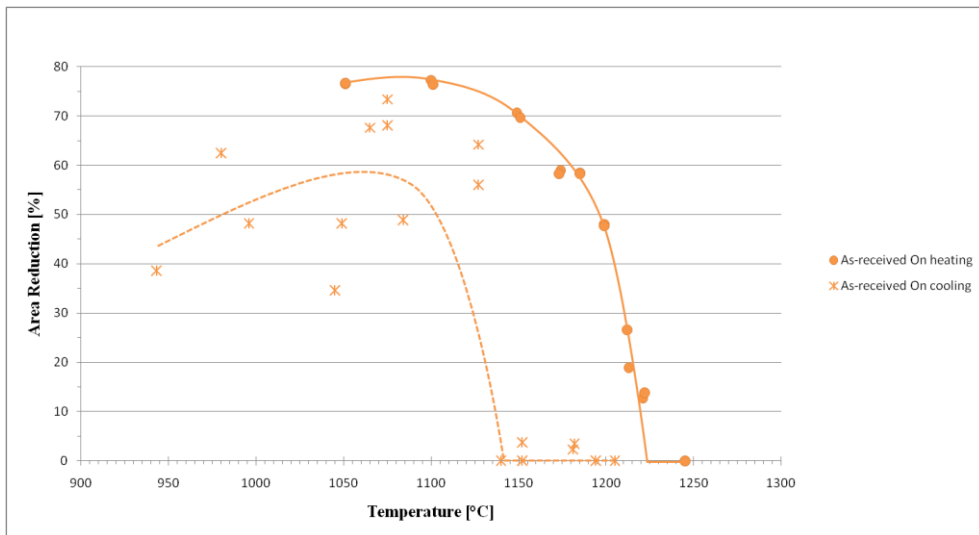


Figure 5. Hot ductility for the as-received condition (grain size ASTM 5, HV 215).

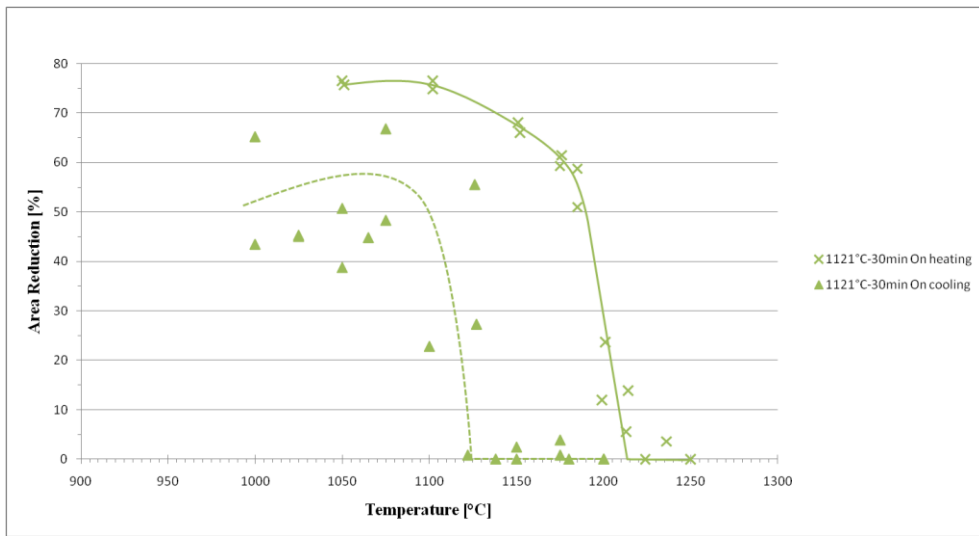


Figure 6. Hot ductility for the “1121°C-30min” condition (grain size ASTM 5, HV 317).

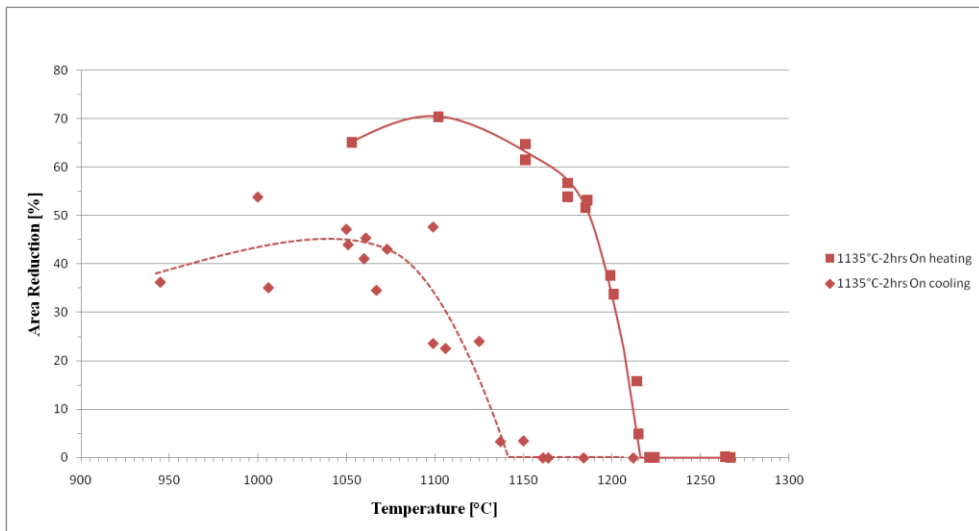


Figure 7. Hot ductility for the “1135°C-2hrs” condition (grain size ASTM 1, HV 283).

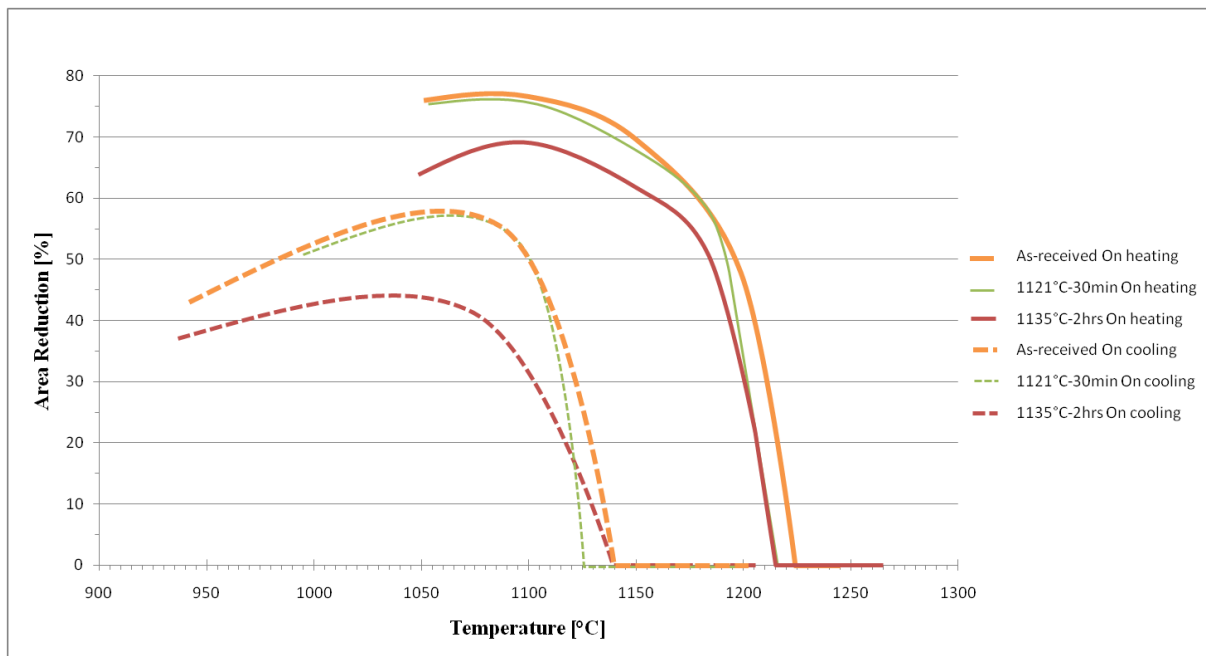


Figure 8. Comparison of the hot ductility for the three conditions

The hot ductility evaluation based on these curves is shown in table 4. It can here, as well as by direct naked eye comparison of the curves, be seen that there is no difference in NDT, DRT or BTR. However, the maximum ductility of the “1135°C/2hrs”-condition is clearly smaller, both for the on-heating and the on-cooling ductility; also the recovery upon cooling is less pronounced for this heat treatment condition which is revealed by the DRR and RDR measurements.

Table 4. Hot ductility parameters determined by Gleeble testing.

	1121°C-30min	As-Received	1135°C-2hrs
Nil Strength Temperature, [°C]	1280	1280	1280
Peak temperature, [°C]	1250	1250	1250
Nil Ductility Temperature, [°C]	1215	1225	1215
Ductility Recovery Temperature, [°C]	1125	1140	1135
Brittle Temperature Range, [°C]	125	110	115
Ductility Recovery Rate, [%]	72	71	54
Ratio of Ductility Recovery, [%]	19	23	16

The liquation mechanism upon heating is likely to be due to the liquation of carbides as seen in Figure 9 for the 1121°C/30min condition as tested at 1185°C.



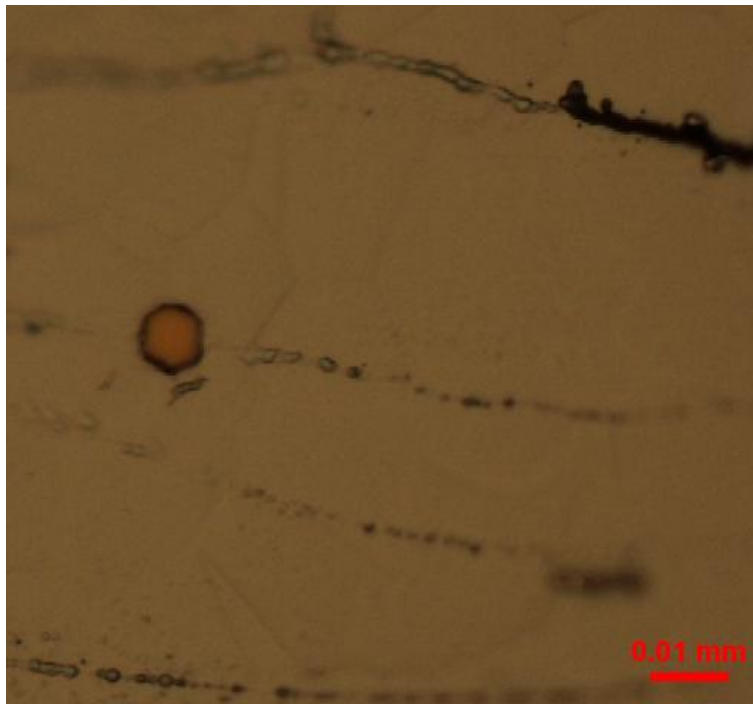


Figure 9. Liquation in grain boundaries during on-heating thermal cycle of “1121°C-30min” condition tested at 1185°C.

Looking closer to the fracture surface on the on-cooling microstructures but at a lower magnification it is clearly seen how eutectic phases decorate the grain boundaries, Figure 10-11.

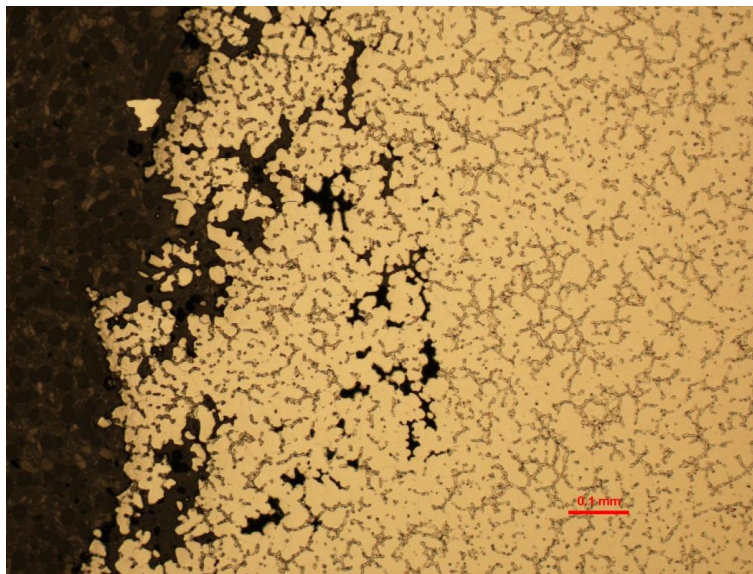


Figure 10. Re-solidified liquid on cooling from 1250°C for the 1121°C-30min condition.

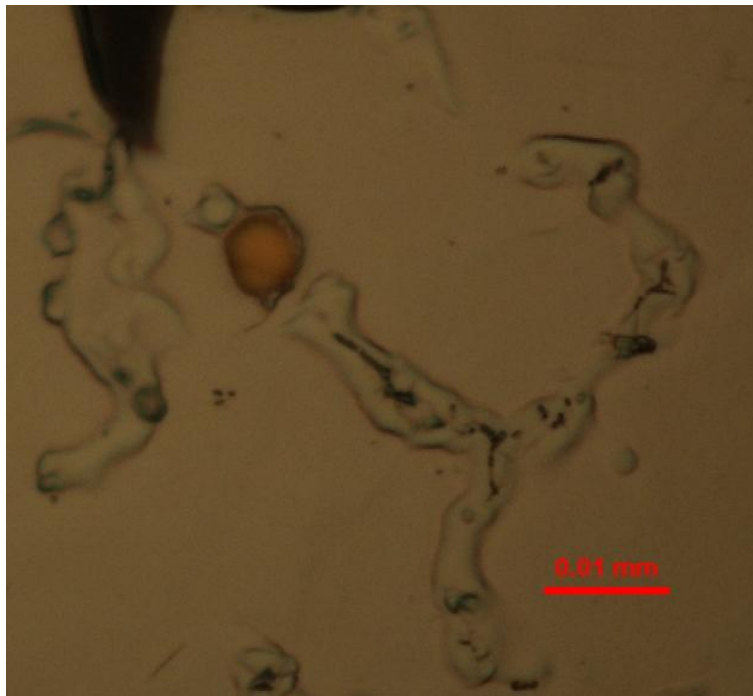


Figure 11. Re-solidified eutectic liquid upon cooling from 1250°C for the 1121°C-30min condition.

In Figures 12-14, cross-section low magnification micro-photos for each specific condition is shown; both for the on-heating and the on-cooling. Generally, it can be seen that for all tested conditions the ductility is large (as measured by the contraction at the fracture surface) for the on-heating samples all the way up to ~1180°C where the ductility drops significantly within a 30°C temperature span. Upon cooling, the ductility starts its recovery at 1140-1130°C and achieves its maximum at approximately 1070°C.

An observation when comparing the three material conditions examined in this study is that the two re-solution heat treated conditions (especially the “1135-2hrs” treatment) seem to be susceptible to nucleation and growth of inter-granular cracks far away from the actual crack surfaces in the on-cooling (not on the on-heating) tests. This intergranular cracking is more pronounced for the coarse grain material and this supports the rationale of the embrittlement caused by liquid eutectic secondary phase constituents. Assuming that the total amount of eutectic produced by carbides is approximately equivalent it is understandable that the ductility of the large grain material with its significantly lower amount of total grain boundary area will be more affected by the same amount of eutectic liquid than the fine grain material. This is consistent with the general acceptance that large grain materials are more susceptible to heat affected zone hot ductility cracking during welding [11].

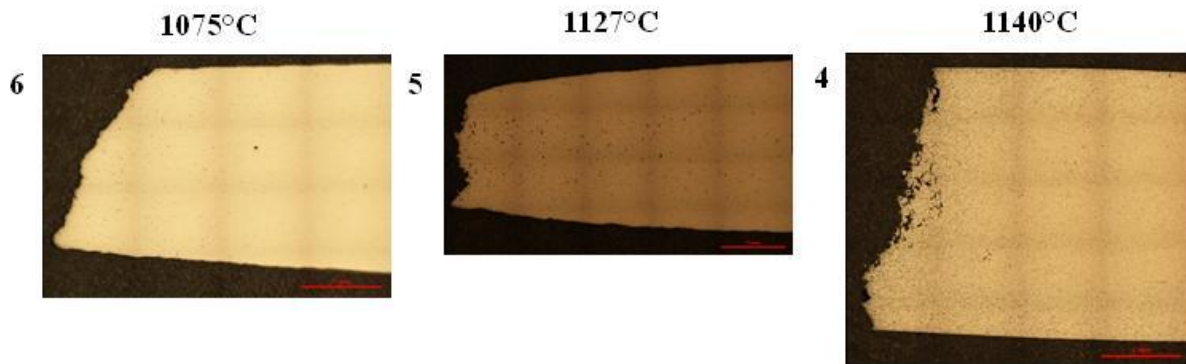
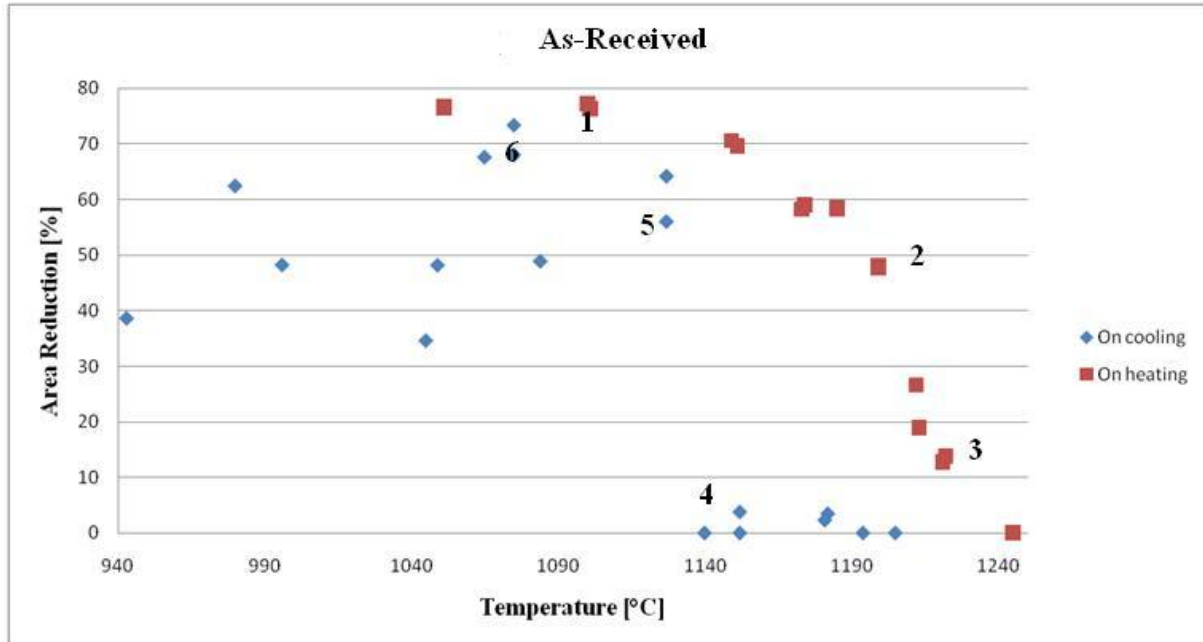
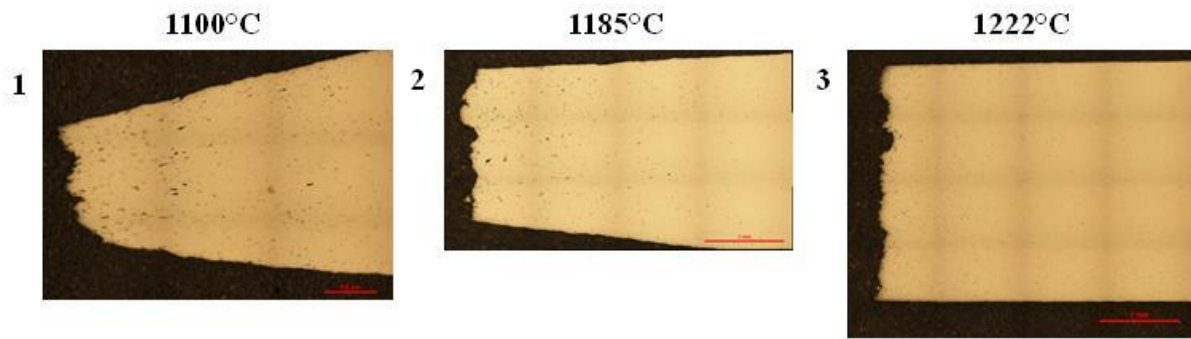


Figure 12. Cross-sectional micro-photographs of selected fractured Gleeble test bars of the as-received material associated with the actual ductility measured on-heating and on-cooling.

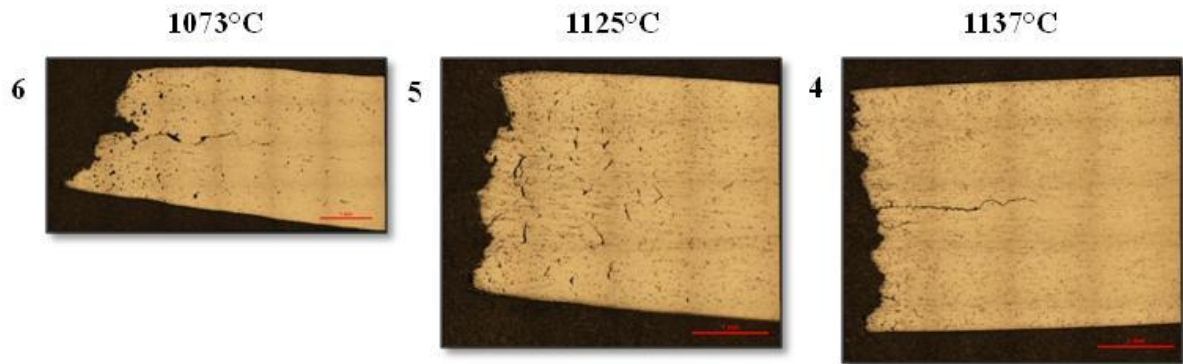
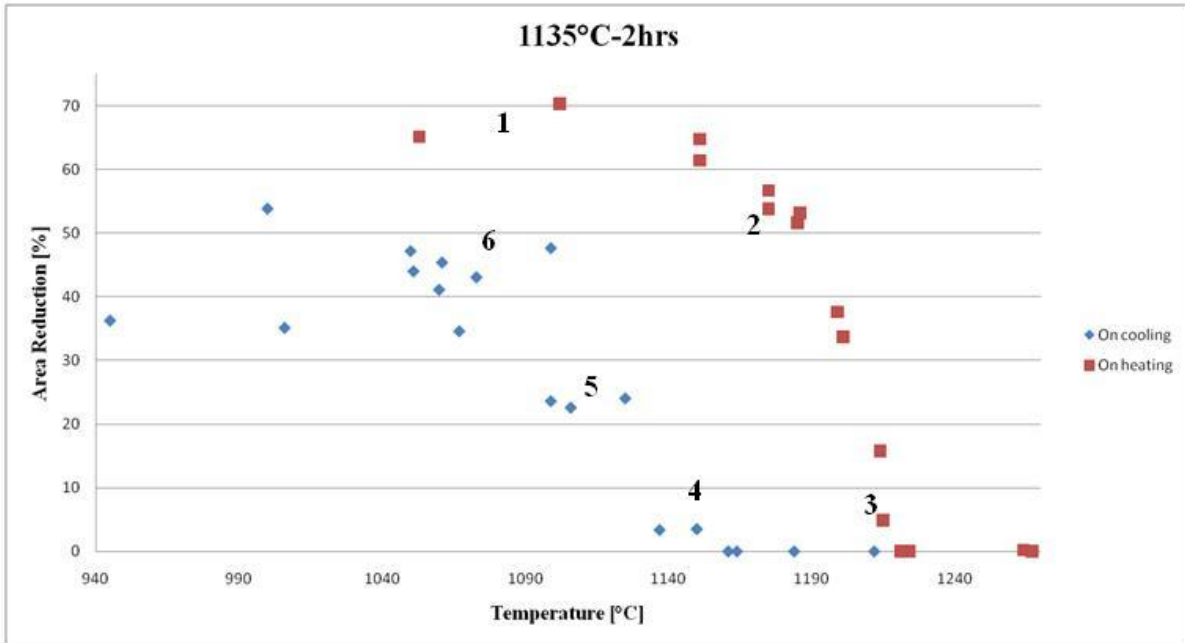
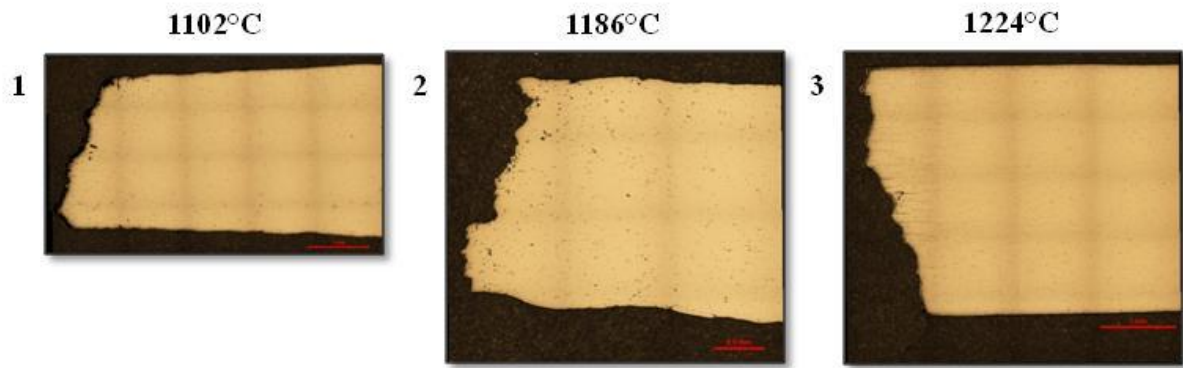


Figure 13. Cross-sectional micro-photographs of selected fractured Gleeble test bars of the 1135°C-2hrs solution material associated with the actual ductility measured on-heating and on-cooling.

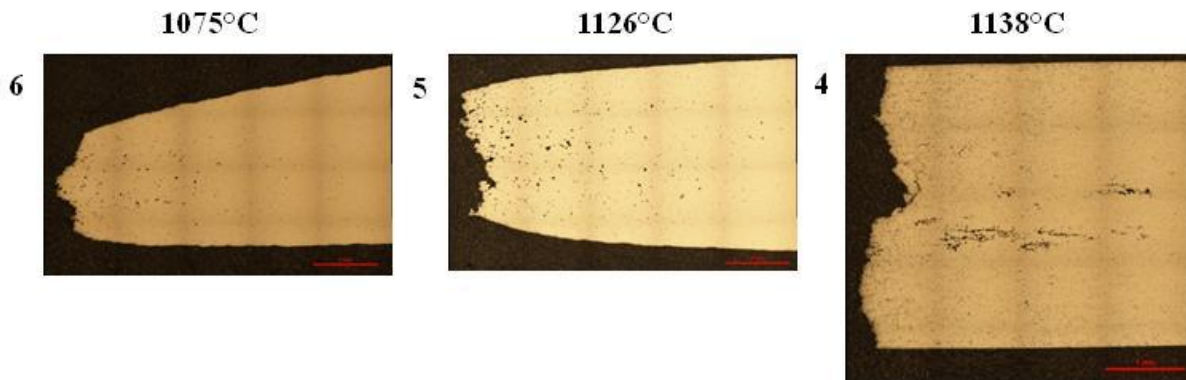
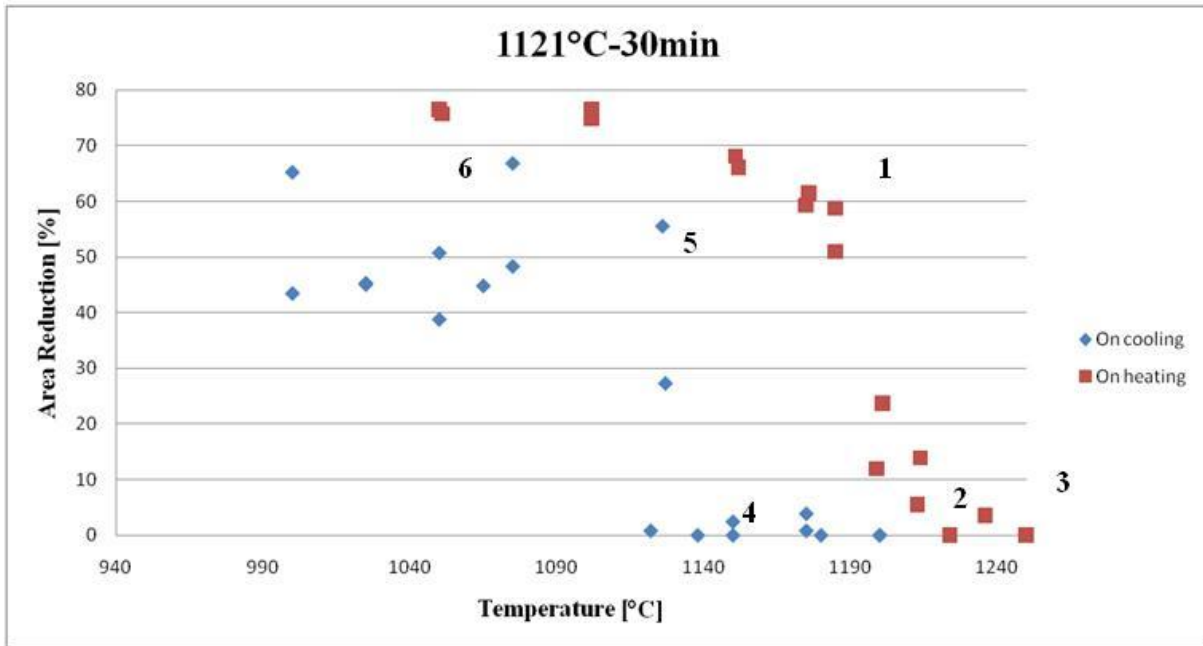
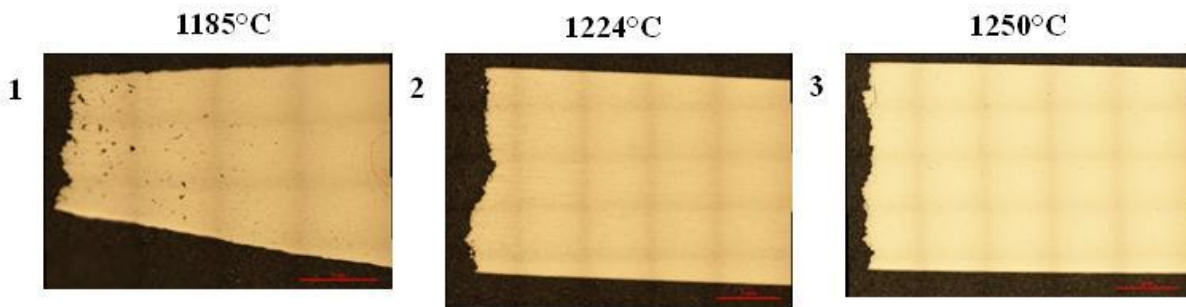


Figure 14. Cross-sectional micro-photographs of selected fractured Gleebale test bars of the 1121°C-30min solution material associated with the actual ductility measured on-heating and on-cooling.

### Discussion

It is obvious from the higher hardness of the re-solution material revealed in figure 4 that a substantial amount of  $\gamma'$  has precipitated during the cooling down from the 1121°C solution heat treatment temperature. The cooling rate was specified to 20°C/min (0.33°C/s) or more down to 500°C which is reasonable in the context of welding large structural components. By simulating

continuous cooling transformation curves using JMatPro material simulation software and 1121°C as the starting point for calculations to match the heat treatments carried out in these studies the precipitation kinetics of  $M_{23}C_6$ ,  $M_6C$  and Gamma-prime were assessed as shown in Figure 15. Although the precipitation kinetics is known to be notoriously difficult to accurately model such simulations still give indications of plausibility. Assuming that the cooling rate would be within the range of 0.1-1°C/s the simulation of the continuous cooling curves and precipitations in Figure 15 indicate that both carbide and ~5%  $\gamma'$  will precipitate after a solution at 1121°C at such cooling rates.

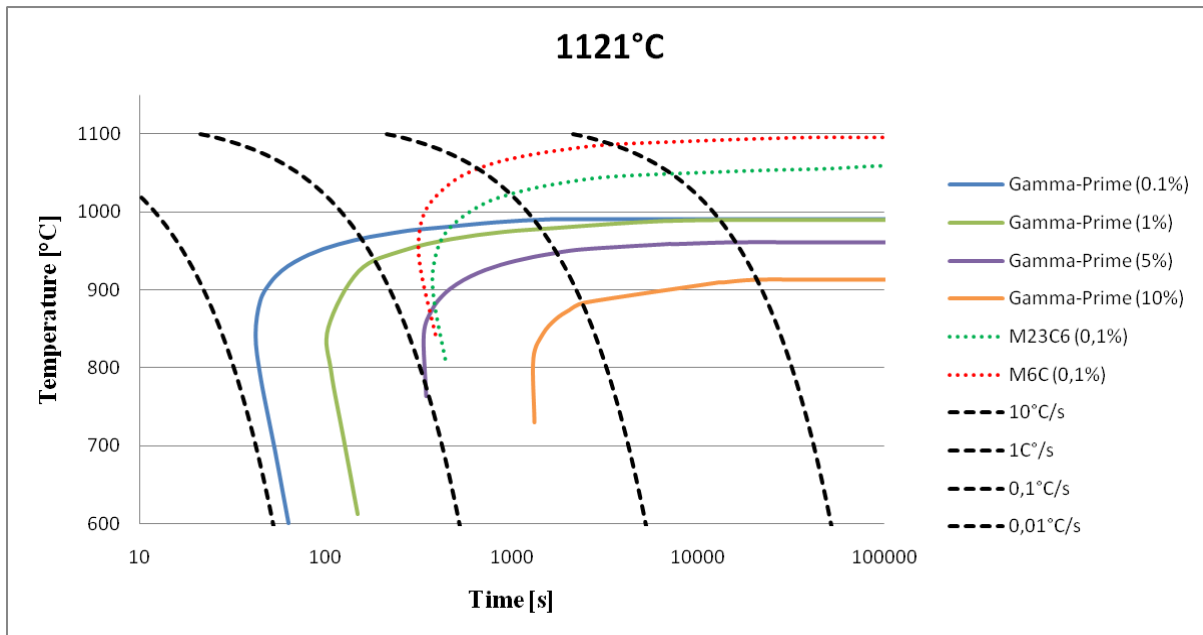


Figure 15. Continuous cooling transformation as simulated by JMatPro simulation for  $M_{23}C_6$ ,  $M_6C$  and  $\gamma'$  when cooling from 1121°C.

However, the large difference in hardness has very little influence on the hot ductility due to the obvious fact that  $\gamma'$  phase may dissolve during the on-heating at ~1000°C. No effect is seen for the on-heating ductility from the coarse grains as evident by comparing 1121°C-30min condition with the 1135°C-2hrs one.

The on-heating ductility drop is a result of liquation of secondary phases and melting point depressant element [5, 9]. Since the Haynes 282 alloy only possesses small amount of these types of constituents it is reasonable to believe that the amount of liquating constituents per grain boundary area is not high enough to significantly affect the on-heating ductility. To determine the exact mechanism it is here necessary to take the advantage of high resolution scanning electron microscopy [12, 13].

As mentioned, the hardness seems to have minor influence on the hot ductility which is generally accepted to govern the susceptibility to HAZ liquation cracks. However, the Gleeble will not be able to account for mechanisms such as backfilling and healing of cracks already nucleated which is a phenomena known to occur [14, 15] and to alleviate (heal) the cracking during welding. Although Gleeble testing is an efficient means of assessing the tendency to hot cracking during welding will never bring the full answer which requires more elaborate and specific testing. It must be emphasized that the hardening response upon cooling down from the solution heat treatment temperature was a bit surprising. Welding of large complex structures where

residual stresses, as high as the yield stresses, easily develop cannot be post-weld heat treated too rapidly (to avoid distortions) which indicate that the age hardening effects, obvious in this study, cannot be neglected. Thus, there is a considerable risk to encounter strain age cracking (SAC) during such heat treatments.

It is therefore believed that the great challenge with this newly developed alloy Haynes 282 may be to avoid the SAC in complex weld designs although the hot ductility is excellent when comparing the BTR (110-125°C for Haynes 282) to other Gamma-prime strengthened superalloys such as Waspaloy (187°C in BTR) and advocates such welding [16].

### Conclusions

1. Alloy Haynes 282 exhibits good hot ductility having a brittle temperature range of 110-125°C for the specific conditions tested in this investigation which advocates good weldability.
2. The hot ductility of the as-received material (bright annealed in a continuous heat treating furnace at 1121-1150°C for about 30min and quenched) is equivalent to that of the low temperature (1121°C) short time (30min) re-solutioned material.
3. Large grain size (ASTM 1) obtained by grain growth at the high temperature (1135°C) long time (2hrs) solution heat treatment lowers the hot ductility compared with the as-received fine grain condition (ASTM 5) by 17% and 7% in terms of ductility recovery rate and ratio of ductility recovery, respectively.
4. A Vickers hardness increase of 103 units during the cooling down heat treatment cycle from the 1121°C solution temperature indicates a risk for strain age cracking at post-weld heat treatments of large welded structures

### Acknowledgements

Professor Lanre Ojo at *the Department of Mechanical and Manufacturing Engineering, University of Manitoba* is appreciated for his input. Dr. Krutika Vishwakarma and Mr. Mike Boskwick, also at *the Department of Mechanical and Manufacturing Engineering, University of Manitoba* are greatly acknowledged for their help in performing the Gleeble tests and in various technical matters related with the Gleeble test equipment. Mr. Daniel Axelsson at *the Department of Materials Technology, Volvo Aero Corporation* is appreciated for help with metallographic preparations. The help from Mr. Stefan Olovsjö at *the Department of Materials- and Manufacturing Technology, Chalmers University of Technology* with JMatPro simulations is greatly acknowledged. Finally, we like to thanks *Haynes International* for providing the material for this study.

### References

1. L. M. Pike, Development of a fabricable Gamma – Prime ( $\gamma'$ ) Strengthened Superalloy, Superalloys 2008 eds. R.C. Reed, K.A. Green, P. Caron, T. P. Gabb, M. G. Fahrman, E. S. Huron, S. A. Woodard, The Minerals, Metals & Materials Society (2008), 191-200.
2. G. Chirieleison, L. Snyder, H. J. White, The Effect of Ageing Heat Treatments on the Mechanical Properties of Nickel Based Superalloy Welds, Proceeding of the 47th Annual Conference of Metallurgists of CIM, Aerospace Materials & Manufacturing: Advances in

Processing & Repair of Aerospace Materials In Honor of Dr. Mahesh Chaturvedi, Winnipeg, Manitoba, Canada, August 24-27 (2008), 223-234.

3. M. Prager, C. S. Shira, Welding of Precipitation- Hardened Nickel- Base Alloys, Welding Research Council Bulletin 128 (1968).

4. R.G. Thompson, J.R. Dobbs, D.E. Mayo, Welding Journal, 65 (1986), 299-304.

5. X. Huang, M.C. Chaturvedi, N.L. Richards, Metallurgical Material Transaction A, 27A (1996), 785.

6. S.C. Ernst, W.A. Baeslack III, J.C. Lippold, Welding Journal, 68 (1989), 418-430.

7. Haynes International Inc., HAYNES<sup>®</sup> 282<sup>®</sup> alloy Product Brochure, 2010.

8. H. J. White, The effect of Aging Heat Treatments on the Mechanical Properties of Nickel Based Superalloy Weld Metal, Proceedings of the Welding and Fabrication Technology for New Power Plants: 1<sup>st</sup> International Electrical Power Research Institute Conference (2008).

9. J. N. DuPont, J. C. Lippold, S. D. Kiser, Welding Metallurgy and Weldability of Nickel-Base Alloys, John Wiley & Sons Inc., USA, 2009, 394-398, 2009.

10. Swedish standards institute, Destructive Tests on Welds in Metallic Materials – Hot Cracking Tests for Weldments – Arc Welding Processes – Part 3: Externally Loaded Tests (ISO/TR 17641-3:2005), 5-9.

11. R. G. Thompson, J. J. Cassimus, D. E. Mayo, J. R. Dobbs, The relationship between grain size and microfissuring in Alloy 718, Welding Journal, 64 (1985), 91.

12. M. Qian, J. C. Lippold, Liquation Phenomena in the simulated heat-affected zone of alloy 718 after multiple post weld heat treatment cycles, Welding Journal, 82 (2003), 145.

13. M. Qian, J. C. Lippold, The effect of rejuvenation heat treatments on the repair weldability of wrought alloy 718, Materials Science and Engineering A, A 340 (2003), 225.

14. C. Huang, S. Kou, Welding Journal, 82 (2003), 184-194.

15. W.F. Savage, D.W. Dickinson, Welding Journal, 51 (1972), 555-561.

16. M. Qian, An Investigation of the Repair Weldability of Waspaloy and Alloy 718 (Ph.D. thesis, The Ohio State University, 2001), 77.